applied optics

# Alignment precision of polarization components

NATHAN HAGEN,[1,*] PRATHAN BURANASIRI,[2] AND YUKITOSHI OTANI[1]

[1]Utsunomiya University, Department of Optical Engineering, Center for Optical Research and Engineering (CORE), 7-1-2 Yoto, Utsunomiya, Tochigi 321-0954, Japan
[2]Department of Physics, Faculty of Science, King Mongkut's Institute of Technology Ladkrabang, Bangkok 10520, Thailand
*Corresponding author: nh@hagenlab.org

Received 8 October 2019; revised 13 November 2019; accepted 14 November 2019; posted 15 November 2019 (Doc. ID 379897); published 11 December 2019

**Recent research publications in the polarization literature have discussed methods of correcting for azimuthal alignment errors of optical elements in postprocessing. However, we show that high angular precision is not difficult to achieve during system alignment, so that postprocessing correction should be unnecessary. We estimate the alignment precision achievable for linear polarizers and waveplates in polarization systems. This shows that using an optical signal model for alignment allows a precision limited by the quality of the optics and detectors rather than the quality of the mechanics, rendering millidegree alignment precision possible with ordinary rotational mounts.** 

https://doi.org/10.1364/AO.58.009750

## 1. INTRODUCTION

Polarizers and waveplates are the fundamental components of polarization instruments, and using the optical extinction properties of crossed polarizers is by far the most common means of aligning the azimuth angles of polarization components in a system. Several recent researchers [1–6] have analyzed how to deal with alignment errors in postprocessing, which begs the question of how precisely we can expect polarization systems to be aligned. Some of these authors discuss alignment errors on the order of 0.5°. Such large errors seem outstandingly bad, but without a quantitative discussion of precision it is difficult to say. In addition, some systems may require achieving errors of $< 0.01°$, and this can be difficult to achieve with standard mounts and methods. In order to address these issues, we estimate the precision that can be achieved during alignment of linear polarizers and waveplates, finding that the techniques for achieving high-precision alignment are not at all difficult. Using the all-optical method that we discuss, one should be able to assemble the components of a polarization system to greater precision than the alignment errors can be detected in postprocessing. Achieving this precision is a matter of using appropriate methods and of careful experimental procedures rather than expensive equipment.

The standard procedure for aligning components in a polarization system is to first set one polarizer ($P_{\text{ref}}$, the reference) at horizontal (0°) to define the orientation axis. All of the remaining components are then aligned to this reference axis. To align a second polarizer $P_2$, we rotate its azimuth angle until we find the point at which the transmitted light through the polarizer pair is a minimum ($P_2$ at 90°) or a maximum ($P_2$ at 0°). These two are the "crossed condition" and "parallel condition." If the desired azimuth angle differs from one of these two, then the usual procedure is to use the indicators on the mechanical mount to adjust the angle to the intended azimuth, so that the precision of the mount will limit the alignment precision. While a typical manual rotation mount often has a vernier precision of about 0.1°, mounts without a vernier are typically limited to precisions of $0.25° \sim 1°$.

Another common procedure requires the use of an electronic stepper-motor rotational stage with a position encoder. As the stepper rotates $P_2$ to a sequence of angular positions, the detector records the transmitted signal at each position. Once a full rotation is completed, we can use the entire sinusoidal signal to calibrate the encoder azimuth. This method relies on the mechanical precision of the stepper motor, so that a mechanical alignment precision between 0.1° and 0.003° is possible, assuming a good optical signal and high performance motors [7]. This technique, however, requires having an electronically controlled rotation stage for every component to be accurately aligned in the system.

Finally, we describe a fourth procedure which depends entirely on the optical properties of Malus's law for alignment. In this procedure, we measure the light level at the crossed and parallel conditions; from these we can use Malus's law to estimate the intensity at the desired azimuth angle of the component. The component is then rotated to the angle at which the target intensity is reached. As this procedure does not rely on mechanical encoding at all, it can achieve a precision limited only by the quality of the optical components. Thus even a coarse mechanical mount can achieve high precision alignment.

For aligning components to angles other than 0° and 90°, we can summarize the four common alignment procedures:

**Procedure 1, crossed condition (⊥)**: rotate $P_2$ to the angle where the minimum light level is reached and set that as the 90° azimuth (error = $\Delta\theta_{\text{bot}}$). If a different angle than 90° is needed, then use the mechanical accuracy of the mount to turn the polarizer from the 90° position to the desired azimuth.

**Procedure 2, parallel condition (∥)**: rotate the polarizer to the position where maximum light level is reached and set that as the 0° azimuth (error = $\Delta\theta_{\text{top}}$). If a different angle is needed, then use the mechanical accuracy of the mount to turn the polarizer from the 90° position to the desired azimuth.

**Procedure 3, sinusoid fitting ("sin"):** using a mount with an electronic encoder, rotate the mount at a series of angles and record the light level at each angular position. After a full rotation, calibrate the azimuth angles of the encoder from the full set.

**Procedure 4, optical method ("opt"):** rotate the polarizer to the position of minimum light, and record that signal as $I_{\text{bot}}$ (error = $\Delta I_{\text{bot}}$). Next rotate the polarizer to the position of maximum light level and record that signal as $I_{\text{top}}$ (error = $\Delta I_{\text{top}}$). Calculate the desired position's light level via $I_{\text{bot}}$ and $I_{\text{top}}$ and the desired azimuth angle, and then rotate the polarizer to achieve that intensity.

Note that the alignment procedures should ideally place the reference polarizer directly in front of the detector and not have the component be aligned between the reference polarizer and detector. The latter setup exposes the detector to changes in the polarization state, so that the detector's polarization dependence (typically on the order of 0.1–1%) introduces an unwanted additional parameter that must be calibrated.

## 2. ALIGNING A LINEAR POLARIZER

Rotating one polarizer in front of another produces a measured intensity given by Malus's law (see Fig. 1) as

$$I(\theta) = I_{\text{b}} + \frac{1}{4} I_0[1 + \cos(2\theta)] + n, \tag{1}$$

where $I_{\text{b}}$ is the bias signal, $I_0$ is the incident light intensity, $\theta$ is the azimuth angle, and $n$ is the measurement noise. Here noise mean $\langle n \rangle = 0$ and noise variance $\text{var}(n) = \langle I \rangle + v_{\text{d}}$, so that $n$ is a mix of Poisson (shot) noise and Gaussian (detector) noise, where $v_{\text{d}}$ is the detector noise variance. Thus, $n$ and $I(\theta)$ are stochastic variables and have units of photoelectrons, while the remainder are deterministic parameters.

When the polarizers are aligned in parallel, we get $I = I_{\text{b}} + \frac{1}{2} I_0 + n_0$, and when crossed we get $I = I_{\text{b}} + n_{90}$. First we consider the noise-free case.

Approximating the cosine curve of Eq. (1) about the peak with a power series gives

$$I_{\text{top}} = I_{\text{b}} + \frac{1}{4} I_0 \left(1 + \left[1 - \frac{1}{2}(2\theta)^2 + \ldots\right)\right]$$

$$\approx I_{\text{b}} + \frac{1}{2} I_0 (1 - \theta^2).$$

For estimating alignment precision, we are interested in analyzing how small changes in intensity ($\Delta I$) depend on small changes in the polarizer angle ($\Delta\theta$). Thus, we can ignore any constant terms and find that the value of $\Delta I$ declines quadratically as $\theta$ moves away from 0°:

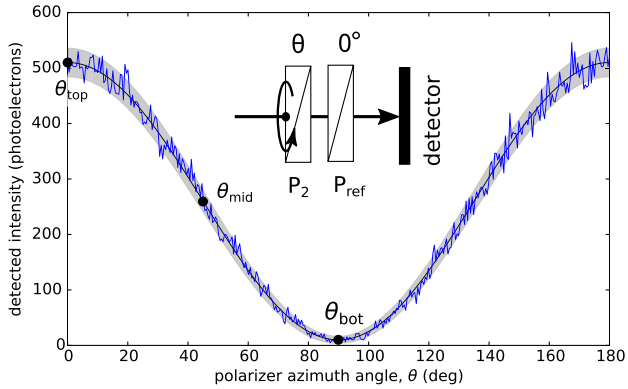


**Fig. 1.** Simulated sinusoidal intensity curve generated by rotating a polarizer in front of a fixed polarizer, showing the noise-free curve (black line), noisy measurement (blue line), and the standard deviation about the noise-free curve (gray region). The parameters assumed are $I_{\text{b}} = 10$, $\sigma_{\text{d}} = 3$, and $I_0 = 500$. *Inset*: the optical alignment layout.

$$[\Delta I]_{\text{top}} = -\frac{1}{2} I_0 (\Delta\theta)^2. \tag{2}$$

From this result, we can see that an angle error of 0.25° creates a fractional intensity change of $\Delta I / I_0 = (0.25\pi/180)^2 = 9.50 \times 10^{-6}$.

Performing the same analysis at the bottom of the sine curve ($\theta = 90°$), we obtain

$$I_{\text{bot}} = I_{\text{b}} + \frac{1}{2} I_0 (\Delta\theta)^2 \tag{3}$$

and

$$\Delta I_{\text{bot}} = \frac{1}{2} I_0 (\Delta\theta)^2. \tag{4}$$

Finally, if we want to align the polarizer to the 45° position (the *middle* of the curve), then a Taylor expansion of about $\theta = \pi/4$ leads to

$$I_{\text{mid}} = I_{\text{b}} + \frac{1}{4} I_0 (1 - 2\Delta\theta) \tag{5}$$

and

$$\Delta I_{\text{mid}} = -\frac{1}{2} I_0 \Delta\theta. \tag{6}$$

Thus, we find a linear dependence instead of quadratic.

For each of these three cases [Eqs. (2), (4), and (6)], we can invert the equations to write the angular sensitivity in terms of changes in intensity:

$$\Delta\theta_{\text{bot}} = \sqrt{2\Delta I / I_0}, \tag{7}$$

$$\Delta\theta_{\text{top}} = \sqrt{-2\Delta I / I_0}, \tag{8}$$

$$\Delta\theta_{\text{mid}} = -2\Delta I / I_0. \tag{9}$$

### A. Incorporating Measurement Noise

At the crossed-polarizer position, the noise variance is given by

$$\mathrm{var}(I_{\mathrm{bot}}) = I_{\mathrm{b}} + v_{\mathrm{d}}, \tag{10}$$

a sum of the Poisson-distributed shot noise due to the detector dark current ("dark shot noise") and the Gaussian-distributed detector noise (variance $v_{\mathrm{d}}$). This assumes that any electronic bias has been subtracted from the measurements prior to applying any variance formulas.

At the parallel (maximum transmission) condition, the measurement intensity is larger, so that the corresponding shot noise is also larger:

$$\mathrm{var}(I_{\mathrm{top}}) = I_{\mathrm{b}} + \frac{1}{2} I_0 + v_{\mathrm{d}}. \tag{11}$$

If we want to estimate the intensity at the $\theta = 45°$ point of the transmission curve, then we can average the maximum and minimum measured intensity values, such that

$$I_{\mathrm{mid}} = \frac{1}{2}(I_{\mathrm{bot}} + I_{\mathrm{top}}), \tag{12}$$

with the resulting variance

$$\begin{aligned}\mathrm{var}(I_{\mathrm{mid}}) &= \frac{1}{2}\mathrm{var}(I_{\mathrm{bot}}) + \frac{1}{2}\mathrm{var}(I_{\mathrm{top}}) \\ &= I_{\mathrm{b}} + \frac{1}{4} I_0 + v_{\mathrm{d}}.\end{aligned} \tag{13}$$

Thus, averaging the peak and valley intensities bears the same variance as an intensity measurement taken at the middle position itself.

Since the crossed and parallel alignment procedures require only locating the minimum or maximum intensities $I_{\mathrm{bot}}$ or $I_{\mathrm{top}}$, we can simply equate the variance of the procedure to that of the single measurement: $\mathrm{var}(I_\perp) = \mathrm{var}(I_{\mathrm{bot}})$, $\mathrm{var}(I_\parallel) = \mathrm{var}(I_{\mathrm{top}})$. The optical procedure, however, requires first estimating $I_{\mathrm{mid}}$ and then using the noisy measurements obtained while searching for the middle position. This doubles the variance to

$$\mathrm{var}(I_{\mathrm{opt}}) = 2I_{\mathrm{mid}} = 2I_{\mathrm{b}} + \frac{1}{2} I_0 + 2v_{\mathrm{d}}. \tag{14}$$

We can now use Eqs. (7)–(9) to calculate the angular standard deviation (for which we use $\epsilon$ in place of $\Delta\theta$) as a function of measurement noise by substituting the measurement standard deviation $\sigma$ for the intensity change $\Delta I$:

$$\epsilon_\perp = \left(\frac{2\sigma_{\mathrm{bot}}}{I_0}\right)^{1/2} = \left(\frac{4\sqrt{I_{\mathrm{b}} + v_{\mathrm{d}}}}{I_0}\right)^{1/2}, \tag{15}$$

$$\epsilon_\parallel = \left(\frac{2\sigma_{\mathrm{top}}}{I_0}\right)^{1/2} \approx \sqrt{2} I_0^{-1/4}, \tag{16}$$

$$\epsilon_{\mathrm{opt}} = \frac{2\sigma_{\mathrm{mid}}}{I_0} = \frac{2\sqrt{8I_{\mathrm{b}} + 2I_0 + 8v_{\mathrm{d}}}}{I_0}, \tag{17}$$

where the approximation in Eq. (16) assumes that the shot noise predominates over detector noise. From these results, we see that while the precision of the parallel condition alignment method (Proc. 2) improves only slowly with increasing SNR, the crossed condition (Proc. 1) and optical methods (Proc. 4) both improve rapidly.

For angles other than 0°, 45°, and 90°, we can use Malus's law in the same way to estimate the target intensity value, and then rotate the component to reach it. While angles between 90° and 45° can achieve high precision using the crossed and optical methods, as one approaches the 0° position (parallel condition) the achievable alignment precision steadily worsens. Section 5 below provides numerical estimates of the precision values we can expect.

In order to help keep track of the quantities discussed here, we review the various labels here. Subscripts "top," "bot," and "mid" refer to the intensities measured while the sinusoidal curve of intensity versus azimuth angle is at its brightest, darkest, or middle point. Subscripts $\perp$, $\parallel$, "sin," and "opt" refer to the alignment procedure used—the crossed, parallel, sinusoid fitting, or optical method.

### B. Alignment Using a Mechanical Encoder

The previous analysis considers the case of manual alignment, with the user manipulating a rotation stage manually to achieve the correct position. A rotational stage that has an electronic encoder or stepper motor, however, allows the user to align the component algorithmically. While this can be done in the same way as for manual alignment, using a binary search procedure to adjust the stage to achieve the desired intensity, a natural procedure for this setup is to collect the sinusoid intensity signal from a full rotation and estimate the azimuth angle corresponding to the motor position. We can expect computer-controlled motion to achieve a precision limited by either the measurement noise (for low signal levels) or by the precision of the rotational stage.

While many researchers have worked on the problem of estimating sinusoid signals in the presence of noise, most of the work deals with independent identically distributed Gaussian (IG) noise rather than Poisson noise. For IG noise, the variance of the angular estimate has been established as [8]

$$\mathrm{var}(\hat{\theta}) = \frac{2v_{\mathrm{G}}}{I_0^2 N}, \tag{18}$$

where $v_{\mathrm{G}}$ is the variance of the Gaussian noise and $N$ the number of measurements. For Poisson-noise corrupted signals, however, this result is useful only when the visibility of the sinusoid signal becomes small, in which case the shot noise can be approximated as uniformly distributed Gaussian noise. Reference [9] develops a more general noise model, with mixed Poisson and Gaussian noise, but does not obtain a closed-form result and focuses on estimating the period of the sinusoid rather than its phase. Although an IG noise model underweighs the low-intensity measurements and overweighs the high-intensity ones, it nevertheless typically provides a reasonable approximation to the Poisson-noise model. Thus, we can give the angular standard deviation for the stepper-motor-based procedure as

$$\epsilon_{\mathrm{sin}} = \left(\frac{2v_{\mathrm{G}}}{I_0^2 N}\right)^{1/2}. \tag{19}$$

### C. Aligning Imperfect Polarizers

The measurement model we have constructed so far [Eq. (1)] assumes that we work with ideal polarizers that transmit 100% of light in the polarizing channel and block 100% of the cross-channel. Real-life polarizers, however, are imperfect diattenuators, which we can model with parameters $q$ and $r$ for the transmission of two orthogonal polarization channels, an ideal polarizer having $q = 1$ and $r = 0$. This gives two degrees of freedom, but we will assume $q = 1$, so that only $r$ determines the extinction ratio $X$ of the polarizer via $X = q/r$. If we assume the two polarizers used for alignment are identical, the measurement model becomes

$$I(\theta) = I_b + \frac{1}{4} I_0[(1+r)^2 + (1-r)^2 \cos(2\theta)]. \quad (20)$$

Almost all polarizer elements have better extinction ratios than 10, so we can safely regard $r$ as small, allowing us to approximate the equation above as

$$I(\theta) \approx I_b + \tfrac{1}{4} I_0[1 + 2r + (1-2r)\cos(2\theta)]. \quad (21)$$

The relation of small changes in intensity to angle therefore becomes

$$\Delta I \approx \frac{1}{4} I_0 (1-2r)\cos(2\Delta\theta), \quad (22)$$

so that all of the angle-sensitivity formulas Eqs. (7)–(9) acquire an extra factor of $(1-2r)$. Moreover, for small $r$, $1/(1-2r) \approx 1+2r$, so that the $\Delta I$ in Eqs. (15)–(17) can be replaced with $(1+2r)\Delta I$. This indicates that it would require a poor polarizer indeed to have a substantial impact on the precision. For example, using a polarizer pair with extinction ratios of 30 reduces the angular sensitivity $\Delta\theta$ (worsens the alignment precision) by a factor of $\sqrt{1+2r} \approx 1.07$ for the "bottom" and "top" configurations, and a factor of 1.14 for the "middle" configuration.

## 3. ALIGNING A LINEAR RETARDER

So far we have analyzed the alignment of a linear polarizer to a reference polarizer. Linear waveplates are also common elements in polarimetry systems, and we should know their alignment precision as well. We start with the most common type of waveplate—a linear quarter-wave retarder.

For a rotating quarter-wave retarder at angle $\theta$ placed between two fixed crossed polarizers (i.e., $P_2$ at 0° and $P_{ref}$ at 90°), we obtain a transmitted intensity of (Fig. 2)

$$I(\theta) = I_b + \frac{1}{4} I_0 \sin^2(2\theta) + n. \quad (23)$$

Taking the same approach as in Section 2, we approximate the equation for small angular deviations about three positions—$\theta_{bot} = 0°$, $\theta_{top} = 45°$, and $\theta_{mid} = 22.5°$—giving the results

$$\Delta I_{bot} \approx 2 I_0 (\Delta\theta)^2, \quad (24)$$

$$\Delta I_{top} \approx -2 I_0 (\Delta\theta)^2, \quad (25)$$

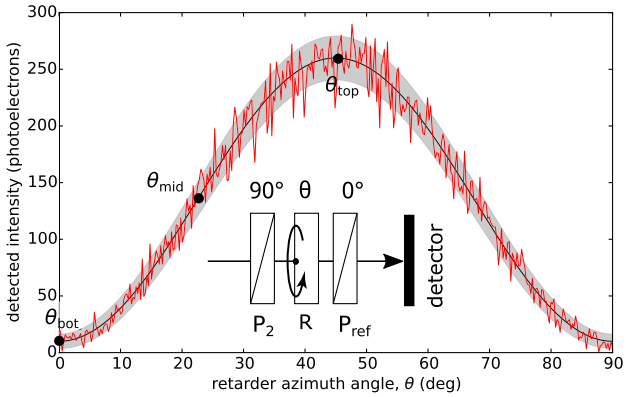


**Fig. 2.** Simulated sinusoidal intensity curve generated by rotating a linear quarter-wave plate $R$ between two crossed polarizers $P_1$ and $P_2$, showing the noise-free curve (black line), noisy measurement (red line), and the standard deviation about the noise-free curve (grey region). The parameters assumed are the same as those used in Fig. 1 : $I_b = 10$, $\sigma_d = 3$, and $I_0 = 500$. *Inset*: the optical alignment layout.

$$\Delta I_{mid} \approx I_0 (\Delta\theta), \quad (26)$$

which converted into small changes in angle give

$$\Delta\theta_{bot} = \sqrt{\Delta I/(2I_0)}, \quad (27)$$

$$\Delta\theta_{top} = \sqrt{-\Delta I/(2I_0)}, \quad (28)$$

$$\Delta\theta_{mid} = \Delta I / I_0. \quad (29)$$

These $\Delta\theta$ values for retarder alignment are all smaller than the corresponding values for polarizer alignment [Eqs. (7)–(9)], so that waveplate alignment should be able to achieve a higher precision than polarizer alignment can.

Next we incorporate noise. The measurement noise variances are the same as in the polarizer case but with the Poisson contribution halved due to the smaller signal level. Thus,

$$\mathrm{var}(I_\perp) = I_b + v_d, \quad (30)$$

$$\mathrm{var}(I_\parallel) = I_b + \frac{1}{2} I_0 + v_d, \quad (31)$$

$$\mathrm{var}(I_{opt}) = 2\left(\frac{1}{2}(I_{bot} + I_{top}) + v_d\right), \quad (32)$$

$$= 2I_b + I_0 + 2v_d. \quad (33)$$

Following the same procedure as for Eqs. (15)–(17), we calculate the waveplate angular error as a function of measurement noise:

$$\epsilon_\perp = (I_b + v_d)^{1/2} (2I_0)^{-1/2}, \quad (34)$$

$$\epsilon_\parallel \approx (2I_0)^{-1/4}, \quad (35)$$

$$\epsilon_{opt} \approx (2I_0)^{-1/2}. \quad (36)$$

These waveplate angle precision values are smaller (i.e., better) than the precision values for polarizer alignment [Eqs. (15)–(17)].

So far we have considered the case of a rotating quarter-wave plate between crossed polarizers. We can also consider the case of aligning the retarder between parallel polarizers. In this case, the intensity varies with waveplate rotation angle as

$$I(\theta) = I_b + \frac{1}{2} I_0[1 + \cos^2(2\theta)] + n. \tag{37}$$

This is the same equation as Eq. (23) but with an added baseline signal of $\frac{1}{4} I_0$. This has no effect on the sensitivity but increases the noise so that the alignment precision will be worse.

When aligning a waveplate, searching for an intensity value gives the appropriate angle to modulus 45°, since any angle $\theta \pm n\pi/4$ produces the same transmitted intensity as the angle $\theta$, for integer $n$. Coarse angular markings on the optical mounts are sufficient to tell a user which azimuth positions correspond to which values for $n$.

In addition to quarter-wave plates, half-wave plates are also common elements. Between crossed polarizers, a half-wave plate produces the following signal as a function of its azimuth angle:

$$I(\theta) = I_b + \frac{1}{2} I_0 \sin^2(2\theta) + n. \tag{38}$$

This is the same equation as Eq. (23) but with twice the factor in front of $I_0$. Thus, a half-wave plate allows better alignment precision than a quarter-wave plate does.

An additional source of error to keep in mind is that when aligning a linear retarder between a pair of crossed polarizers, any alignment error in the polarizers will naturally bias the alignment in the retarder as well. A quarter-wave plate placed between crossed polarizers generates an intensity at the detector of

$$\begin{aligned} I(\theta) &= 1 - \cos(2\Delta)\cos^2(2\theta) - \sin(2\Delta)\sin(2\theta)\cos(2\theta) \\ &\approx 1 - \cos^2(2\theta)[1 - 2\Delta\ \sin(2\theta)] \end{aligned} \tag{39}$$

for retarder azimuth $\theta$ and (small) polarizer azimuth error $\Delta$. Thus, a polarizer that is misaligned by 1° from its nominal crossed-polarization position will in turn bias the alignment of the linear waveplate by approximately twice the same angle—2°—for quarter-wave plate azimuth angles near 0°.

## 4. ALIGNING HIGH-ORDER LINEAR RETARDERS

High-order linear retarders are used in channeled spectropolarimetry [10,11] for detecting spectrally resolved polarization. These systems use spectra and not just single intensity values, so that the transmission of this setup varies with wavelength. Figure 3 shows the amplitude modulation resulting from placing a high-order waveplate between crossed polarizers, for fast-axis orientation angle $\theta$ from 0° to 45° and for a Gaussian-shaped spectrum. At 0°, there is no modulation in the spectrum, so that the integrated intensity across the spectrum is a minimum, just as for the quarter-wave plate. As the fast axis azimuth increases towards $\pi/4$, the modulation amplitude approaches its maximum, so that the integrated intensity across the spectrum is also a maximum. Above 45°, the modulation contrast begins to decrease once again, in the same pattern as in Fig. 2. Thus, if we integrate the signal across the spectrum, we can treat the high-order retarder alignment in exactly the same way that we treat the quarter-wave plate's alignment.

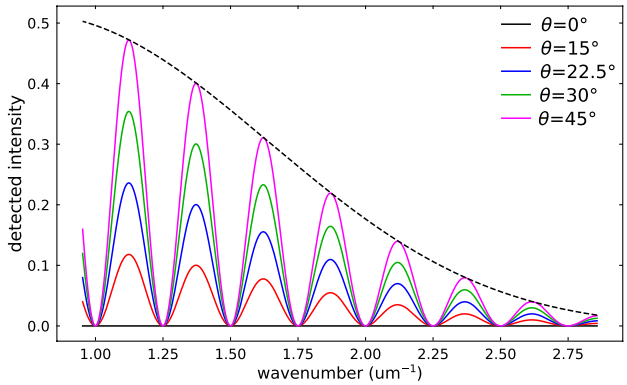


**Fig. 3.** Simulated incident spectrum transmitted by a 0.5 mm thick quartz retarder placed between crossed polarizers, across the 350–1050 nm spectral range. Each of the curves indicates a different azimuth angle for the retarder, while the dashed black curve indicates the envelope of the intensity spectrum.

To show this, we can write the expression for the intensity transmitted by the high-order retarder between crossed polarizers,

$$I(\delta, \theta) = I_b + \frac{1}{4} I_0 - \frac{1}{4} I_0[\cos^2(2\theta) + \cos(\delta(\lambda))\sin^2(2\theta)] + n, \tag{40}$$

where retardance $\delta(\lambda)$ is wavelength-dependent. The integral of this spectrum gives

$$\begin{aligned} I(\theta)s &= \frac{1}{\lambda_{max} - \lambda_{min}} \int_{\lambda_{min}}^{\lambda_{max}} I(\delta(\lambda), \theta) d\lambda \\ &\approx I_b + \frac{1}{4} I_0'[1 - \cos^2(2\theta)] + n, \end{aligned} \tag{41}$$

which is equivalent to drawing a curve halfway between the upper (black-dashed curve) and lower (solid black line) envelopes shown in Fig. 3, producing an expression equivalent to Eq. (23).

## 5. QUANTITATIVE ALIGNMENT PRECISION ESTIMATES

Providing experimental validation of the expressions of Sections 2 and 3 is difficult, since it requires equipment that has a higher precision than the optical method does. This can be quite hard to come by. However, our experience has been that using the optical approach (Procedure 4) in place of Procedure 1 (i.e., the crossed condition followed by using rotation mount indicators) has noticeably improved our measurements.

To make the results more concrete, we can calculate the expected angular precision that can be achieved if we use a typical modern scientific detector array to align a polarizer using optical-only methods to positions of 0°, 90°, and 45°. To start,

we assume detector pixels with a full well capacity of 50,000 electrons (typical for 6 μm pixels), a read noise $\sigma_d$ of 15 electrons, and a mean dark current signal of 10 electrons. We will ignore the dark current itself by assuming that the frames are background-subtracted but keep the dark current shot noise. We assume that the integration time of the detector is set to achieve a maximum signal at 90% of full well capacity, i.e., $I_0 = 45{,}000$ electrons. Calculating the angular precision for our three alignment approaches, we use Eqs. (15)–(17) to obtain

$$\epsilon_\perp = 2(15^2 + 10)^{1/4}(45{,}000)^{-1/2} = 0.037 \text{ rad} = 2.1°,$$

$$\epsilon_\parallel = 2^{1/2}(45{,}000)^{-1/4} = 0.097 \text{ rad} = 5.6°,$$

$$\epsilon_{opt} \approx 2^{3/2}(45{,}000)^{-1/2} = 0.13 \text{ rad} = 0.76°.$$

These initial estimates, however, are unrealistic in that they ignore our ability to average (or sum) together many measurements. For the case of Poisson noise, this increases the detected signal faster than it does the noise. In the lab, we are also usually free to increase the intensity of the light source, by a factor approaching the extinction ratio of the polarizer pair—$10^6$ for good polarizers. This is the real strength of the crossed-polarizer condition. The parallel and midpoint conditions are not free to increase the light level, since doing so leads to detector saturation. Finally, in the above model we have also assumed a single 6 μm pixel, and most systems provide a much larger detection area than that.

For a more reasonable model, we modify the setup to allow temporal summing over 100 measurements, spatial summing over a $100 \times 100$ array of pixels, and a $10^4\times$ boost in the illumination level for the crossed condition; then, we obtain

$$\epsilon_\perp = 2[(1.5 \times 10^7)^2 + 1.0 \times 10^7]^{1/4}(4.5 \times 10^{14})^{-1/2}$$
$$= 0.37 \text{ mrad} = 0.021°,$$

$$\epsilon_\parallel = 2^{1/2}(4.5 \times 10^{10})^{-1/4} = 3.1 \text{ mrad} = 0.18°,$$

$$\epsilon_{opt} \approx 2^{3/2}(4.5 \times 10^{10})^{-1/2} = 0.013 \text{ rad} = 0.00076°.$$

Not only does this quantify the conventional wisdom that crossed-polarizer alignment achieves a much better precision than the parallel condition can, but we also see that alignment at 45° using the all-optical method can achieve a higher precision that the cross-condition can. Moreover, with careful measurements, there is still considerable room to improve on even these millidegree precision values. Precision commercial mechanical stepper motor stages, on the other hand, are capable of achieving absolute accuracy down to only about 3 mdeg, even though their step sizes are smaller ($0.2 \sim 0.3$ mdeg) [7].

For a second example alignment setup, we consider using a photodiode detector with a HeNe laser light source to align a quarter-wave plate to azimuth angles of 0°, 22.5°, and 45°. These correspond to the crossed, mid, and parallel condition respectively, modeled in Eqs. (34)–(36). The photodiode we consider is a Thorlabs FDS100, with a stated noise-equivalent power (NEP) of $1.2 \times 10^{-14}$ W · Hz$^{1/2}$ at $\lambda = 900$ nm, a responsivity of 0.65 A/W at $\lambda = 980$ nm, and a dark current of 1 nA. For operating at 900 nm, the responsivity drops to about 0.61 A/W, and at the HeNe laser wavelength of 633 nm, the responsivity drops further to about 0.49 A/W. If we apply a frequency-domain filter to the output equivalent to integrating the signal over a half second of time, then the equivalent bandwidth of the output will be 1 Hz, for an NEP of $1.2 \times 10^{-14}$ W. For the source, we consider Thorlabs' HNL020RB HeNe laser, which has an optical output of 2 mW. As a result, the parameters for our formulas are

$$I_0 = (2 \times 10^{-3} \text{ W})(0.49 \text{ A/W})(0.5 \text{ s})(6.25 \times 10^{18} \text{ e}^-/\text{s})$$
$$= 3.06 \times 10^{15} \text{ photoelectrons},$$

$$I_b = (1 \text{ nA})(0.5 \text{ s})(6.25 \times 10^{18} \text{ e}^-/\text{s}) = 3.13 \times 10^9 \text{ electrons},$$

$$v_d = (1.2 \times 10^{-14} \text{ W·Hz}^{1/2})(1 \text{ Hz})(0.61 \text{ A/W})$$
$$\times (6.25 \times 10^{18} \text{ e}^-/\text{s}) = 4.58 \times 10^4 \text{ electrons}.$$

Since the detector noise $v_d$ is negligible in comparison to the photon shot noise and dark current shot noise, Eqs. (34)–(36) give the estimated alignment precisions as

$$\epsilon_\perp \approx (3.13 \times 10^9)^{1/2}(6.25 \times 10^{18})^{-1/2} = 2.23 \times 10^{-5} \text{ mrad}$$
$$= 1.28 \text{ mdeg},$$

$$\epsilon_\parallel = 2(6.25 \times 10^{18})^{-1/4} = 4.00 \times 10^{-5} \text{ mrad} = 2.29 \text{ mdeg},$$

$$\epsilon_{opt} \approx 2(6.25 \times 10^{18})^{-1/2} = 7.98 \times 10^{-10} \text{ rad} = 45.7 \text{ ndeg}.$$

The precision estimated for the optical alignment method when setting the waveplate to the 22.5° position is given in nanodegrees. Clearly, the alignment precision here will be limited entirely by the mount and by deviations from the measurement model, such as waveplate and polarizer nonuniformities, rather than by noise. For the crossed and parallel alignment methods for setting the waveplate to positions of 0° and 45°, we see that there is surprisingly only a factor of 2 difference between them due to the high dark current that this system suffers. Thus, this photodiode is well-suited to bright illumination applications.

## 6. CONCLUSIONS

Although the alignment of polarization component azimuth angles is a straightforward process, the recent research literature has shown that it is not generally known what alignment precision we should expect. A number of researchers have shown how to correct for polarization component alignment errors in postprocessing, but our precision analysis indicates that researchers' efforts are better directed at getting the alignment precise in the first place, during system assembly. Taking advantage of the quality of polarization optics and using the optical signal as a guide, a patient technician should have no great difficulty in achieving millidegree-order alignment errors, so that expensive mechanical mounts and precision electronic encoders are unnecessary. In addition, we have shown that the conventional crossed-polarized method does not achieve the highest precision possible when the source light level is fixed. Aligning a polarizer to the 45° position, or a waveplate to the

22.5° position, allows for greater precision for fixed source light. If one has the freedom to increase the source intensity as desired, then the crossed-polarization condition may be more accurate.

While alignment precision at the millidegree level therefore appears to be relatively easy to achieve in principle, precision at this level is also difficult to assess. Higher-order effects such as polarizer and retarder spatial nonuniformity will begin to play a significant role. Higher-order mechanical problems in the mounts also become problematic, such as eccentricity error (radial runout) in the rotational stage and wobble in the stage's rotational axis.

The discussion above has focused on linear polarizers and linear waveplates, but more complex polarization elements certainly exist. One commonly found such element is a "biplate" retarder, typically constructed by cementing two retarders with their azimuth angles rotated by 90° from one another [12]. Each of the two constituent waveplate components is high-order linear retarders and thus can be aligned using the methods suggested in Section 4. If the azimuth angles of the two plates are not quite aligned to one another, however, the result is an element that has a fast axis whose azimuth angle varies with wavelength [13]. Aligning composite elements such as this require building a measurement model describing how the element azimuth angle affects the detected intensity.

**Funding.** King Mongkut's Institute of Technology Ladkrabang (Academic Melting Pot Fellowship 2019).

**Disclosures.** The authors declare no conflicts of interest.

## REFERENCES AND NOTES

1. T. Mu, C. Zhang, C. Jia, W. Ren, L. Zhang, and Q. Li, "Alignment and retardance errors, and compensation of a channeled spectropolarimeter," Opt. Commun. **294**, 88–95 (2013).
2. H. Dai and C. Yan, "Measurement errors resulted from misalignment errors of the retarder in a rotating-retarder complete Stokes polarimeter," Opt. Express **22**, 11869–11883 (2014).
3. B. Yang, X. Ju, C. Yan, and J. Zhang, "Alignment errors calibration for a channeled spectropolarimeter," Opt. Express **24**, 28923–28935 (2016).
4. N. C. Bruce, J. M. López-Téllez, O. Rodríguez-Núñez, and O. G. Rodríguez-Herrera, "Permitted experimental errors for optimized variable-retarder Mueller-matrix polarimeters," Opt. Express **26**, 13693–13704 (2018).
5. X. Ju, C. Yan, J. Zhang, B. Yang, and W. Xing, "Adaptive correction of retardations with immunity to alignment errors for a channeled spectropolarimeter," Appl. Opt. **57**, 8134–8142 (2018).
6. W. Xing, X. Ju, C. Yan, B. Yang, and J. Zhang, "Self-correction of alignment errors and retardations for a channeled spectropolarimeter," Appl. Opt. **57**, 7857–7864 (2018).
7. Rotational stage specifications are from two example motorized stages—the URS100 series from Newport Corp. (www.newport.com) and the M-062 from Physik Instrumente GmbH (http://www.pi-usa.us). Note that for these specifications we need to be careful to differentiate between the motor stepsize (0.2 mdeg for the URS100, 0.3 mdeg for the M-062) and the absolute accuracy of the stage, which include effects of repeatability error. The latter is always larger: 8 mdeg for the URS100, 3 mdeg for the M-062.
8. T. Andersson and P. Händel, "IEEE standard 1057, Cramér-Rao bound and the parsimony principle," IEEE Trans. Instr. Meas. **55**, 44–53 (2006).
9. C. Li and Y. Zhu, "Cramer-Rao bound for frequency estimation of spectral interference and its shot noise-limited behavior," IEEE J. Sel. Top. Quantum Electron. **23**, 410–416 (2017).
10. K. Oka and T. Kato, "Spectroscopic polarimetry with a channeled spectrum," Opt. Lett. **24**, 1475–1477 (1999).
11. N. Hagen, K. Oka, and E. L. Dereniak, "Snapshot Mueller matrix spectropolarimeter," Opt. Lett. **32**, 2100–2102 (2007).
12. B. Boulbry, B. L. Jeune, J. C. F. Pellen, and J. Lotrian, "Identification of error parameters and calibration of a double-crystal birefringent wave plate with a broadband spectral light source," J. Phys. D **35**, 2508–2516 (2002).
13. H. Gu, X. Chen, H. Jiang, C. Zhang, W. Li, and S. Liu, "Accurate alignment of optical axes of a biplate using a spectroscopic Mueller matrix ellipsometer," Appl. Opt. **55**, 3935–3941 (2016).